Structure and properties of clay/recycled plastic composites

Istrate, O., & Chen, B. (2018). Structure and properties of clay/recycled plastic composites. *Applied Clay Science*, *156*, 144-151. https://doi.org/10.1016/j.clay.2018.01.039

Published in:
Applied Clay Science

Document Version:
Peer reviewed version

Structure and properties of clay/recycled plastic composites

Oana M. Istrate[a,1] and Biqiong Chen[b,*]

[a]Department of Mechanical and Manufacturing Engineering and Trinity Centre for Bioengineering, Trinity College Dublin, Dublin 2, Ireland

[b]School of Mechanical and Aerospace Engineering, Queen's University Belfast, Belfast BT9 5AH, United Kingdom

[*]Corresponding author. Email: b.chen@qub.ac.uk

[1]Current address: National Graphene Institute, School of Materials, University of Manchester, Manchester M13 9PL, UK

We are presenting a clay (montmorillonite) based method of reintroducing plastics back into the market without subjecting them to extended processing methods. We have prepared montmorillonite/recycled polymer materials with recycled polystyrene (R-PS) and recycled polyethylene (R-PE). R-PS was melt mixed with as-received organomodified montmorillonite or blowing agent treated organomodified montmorillonite which led to intercalated/exfoliated clay/polymer nanocomposites. Similarly, R-PE was melt compounded, with or without the addition of a compatibiliser with the above mentioned organomodified clay minerals which resulted in conventional composite formation. In the case of R-PS, the thermal degradation temperature of the materials increased with the presence of clay minerals, whereas for R-PE based materials it was observed that the thermal degradation temperatures decreased with the presence of clay minerals. Overall it was observed that the presence of clay minerals improved the stiffness of the materials. The use of blowing agent treated organomodified clay minerals in R-PS led to nearly doubled impact strength compared to organomodified clay/R-PS nanocomposites.

Keywords: Plastics; Clay minerals; Nanocomposites; Thermal properties; Mechanical properties; Recycling;

1 Introduction

During the life cycle of a plastic material and depending on the environment in which the material is used, the polymer may undergo thermo- and/or photo-oxidative degradation, leading to irreversible changes at molecular and morphological levels (Kartalis et al., 2001; Pospíšil et al., 1995). These changes to the structure of the polymer are typically more pronounced when material recovery is performed. Mechanical recycling is an energy effective plastics recovering process that uses mechanical processes (e.g. separation, washing, shredding and processing) to recover polymeric materials from the recycled plastic stock (Finnveden et al., 2005; Vilaplana and Karlsson, 2008). However, the mechanically recycled polymers are typically characterised by inferior mechanical properties, compared to the pristine materials (Kartalis et al., 2001), which may be due to thermo-mechanical deterioration that may occur during the recovery process (Strömberg and Karlsson, 2009; Vilaplana and Karlsson, 2008).

Thermo-oxidative and thermo-mechanical degradation of polymer chains and the possible presence of unwanted degraded chemical substances make interesting the use of additives that are able to minimise the impact of these undesirable products. Over the years, a myriad of materials (such as: stabilisers, compatibilisers and particles) have been used in order to diminish the impact of thermo-oxidative and thermo-mechanical degradation experienced by the plastic materials (Fortelný et al., 2004; Vilaplana and Karlsson, 2008). The well-known ability of clay minerals to adsorb and absorb chemical substances and the beneficial improvement of thermal, mechanical and barrier properties with the dispersion of small amounts of clay minerals in pristine polymers and polymer blends make clay an ideal candidate to aid in the recovery of plastic materials (Chaiko and Leyva, 2005; Katti et al., 2006; Lee et al., 1997; Liu et al., 2000; Okada and Usuki, 2007; Zhao et al., 2005).

Clay minerals are ubiquitous in nature, have the ability to absorb harmful substances that might be present in the recycled stock and each clay layer is characterised by superior strength and stiffness compared to any polymer matrix (Chen and Evans, 2006). The effects of adding natural bentonite (i.e., sodium montmorillonite, Cloisite® Na) or organomodified bentonite (i.e., Cloisite® 25A) in recycled polyethylene terephthalate (PET) have been structurally and mechanically evaluated for different clay mineral loads (Pegoretti et al., 2004). It was observed that the dispersion of organomodified bentonite resulted in intercalated clay nanostructures, whilst natural bentonite presented mostly as aggregates. The

tensile properties showed that the modulus increased with clay minerals load augmentation and the tensile strength climaxed at 5 wt.% clay regardless of the type of clay mineral used (Pegoretti et al., 2004). The formation of intercalated and exfoliated nanostructures increases the exposure of the surface of the clay layers and allows for the stress to which polymer matrix is subjected to transfer to the nanostructure so as to withhold superior loads. The effect of 5 wt.% organomodified bentonite dispersion into another recycled polyester, i.e., poly(butylene terephthalate) (PBT) has also been investigated (Quispe et al., 2015). It was observed that the type of organic modifier influences the morphology of the polymer nanocomposite. Partially exfoliated clay/polymer nanocomposites were obtained when using single tail tallow (i.e., Cloisite® 25A) and only intercalated nanostructures occurred when a double tail tallow (i.e., Cloisite® 20A) was used. The partially exfoliated nanocomposites presented a better dispersion of the nanofiller and the higher improvements in the tensile modulus and the tensile strength over recycled PBT when compared to intercalated Cloisite® 25A/PBT nanocomposites (Quispe et al., 2015). The dispersion of organomodified bentonite (i.e., Cloisite® 30B) into recycled polypropylene with 30 wt.% maleated polypropylene led to the formation of well dispersed composite materials characterised by highly intercalated nanostructures (Phuong et al., 2008). The mechanical properties showed progressive improvements with smectite augmentation with the highest values for tensile strength and Charpy impact strength being encountered for a clay load of 4 wt.% (Phuong et al., 2008).

Analysing the average waste consumption of a household, it was discovered that thermoplastic waste represented 12% of the yearly household residue; from which polyethylene (PE) made up 75% and polypropylene (PP), polystyrene (PS), polyvinyl chloride (PVC) and PET represented 10, 8, 4 and 3%, respectively (Finnveden et al., 2005). Thus, the current study focuses on two major household waste thermoplastics, a non-polar polymer, i.e., PE, and a low-polar polymer, i.e., PS. This work examines the structure and thermal and mechanical properties of clay/recycled polymer composites manufactured with an as-received organomodified montmorillonite (Organoclay Nanomer® I.44P) and a blowing agent-treated organomodified montmorillonite. These treated clay minerals have been previously used to manufacture clay/polymer nanocomposites with a higher degree of exfoliation and superior properties (Istrate and Chen, 2014). It is hypothesised that by dispersing these clay minerals in recycled polymer matrices polymer composites/nanocomposites with better clay dispersion and superior properties will form. If this is the case, we hope that by using this procedure higher amounts of plastics will be recycled

and reintroduced to the market and that the versatility of the products manufactured with recycled polymers will increase.

2 Experimental section

2.1 Materials

Recycled high-density polyethylene (R-PE) from Monnad Industries (Ireland), obtained from pelletizing milk jugs, was generously provided by Athlone Institute of Technology (Ireland). Recycled impact-modified polystyrene (Axpoly® PS01), denoted from here on as R-PS and representing 100% post-consumer recycled polymer recovered from refrigerators, was generously supplied by Axion Polymers (UK). R-PE and R-PS were used as polymer matrices for the manufacturing of clay/polymer composites. For R-PE a compatibilising agent, i.e., polyethylene-grafted-maleic anhydride (PEgMA) was used. PEgMA was purchased from Sigma-Aldrich Ireland Ltd. (Ireland). Organomodified montmorillonite Nanomer® I.44P (Clay), a dimethyl dihydrogenated tallow ammonium chloride (2M2HTA) modified montmorillonite, manufactured by Nanocor Corporation (USA), was kindly supplied by Nordmann, Rassmann GmbH (Germany). The organic content of the organomodified montmorillonite was previously determined from loss on ignition test to be 40% (Istrate et al., 2012). The as-received organomodified montmorillonite was treated with azodicarboxamide (ADC), a well-known blowing agent, following a procedure described in our previous publication (Istrate and Chen, 2014). The resulting clays were denoted as ADC-Clay.

2.2 Nanocomposite manufacturing

R-PS, R-PE and compatibilised R-PE (R-PE/PEgMA = 90/10, w/w) with 4 wt% clay layers were manufactured on a Prism twin screw extruder (UK) with 16 mm-diameter screws and a length to diameter ratio of 25. The materials were passed three times through the twin-screw, once at a screw speed of 200 rpm and then twice at a screw speed of 100 rpm. For the organomodified montmorillonite nanocomposites the temperatures were maintained at 160, 170, 175, and 180 °C from hopper to die, for all three processes. For the blowing agent-treated organomodified montmorillonite the temperatures were maintained at 160, 170, 175, and 180 °C when the material was processed at 200 rpm and increased to 165, 175, 190, and 200 °C when the material was processed at 100 rpm. After passing the material through the extruder, the extrudates were water cooled and pelletized. Tensile and impact specimens were

manufactured on a bench top injection moulder (Ray Ran model 2 Test Sample Injection Moulding Apparatus, UK). The injection moulder was used at a barrel temperature of 220 °C, a tool temperature of 55 °C and a pressure of 0.76 MPa for R-PE materials and a barrel temperature of 210 °C, a tool temperature of 55 °C and a pressure of 0.76 MPa for R-PS materials.

2.3 Characterization

X-ray diffraction (XRD) was carried out on a Phillips PW1720 X-Ray Diffractometre with a $CuK\alpha_1$ (λ=0.15406 nm) anode tube at standard conditions of 40 kV and 20 mA. The samples were tested from 2º to 10º, 2θ angle, at a step size of 0.02º and a duration of 2.5 s per step. Powder samples were used for the clay minerals, while thin samples (1 mm thick) were used for the composite materials. These samples were prepared by applying a pressure of 5.1 MPa for 10 s at 210 ºC.

Transmission electron microscopy (TEM) was performed on a TECNAI G2 20 Twin electron microscope at 200 kV accelerating voltage. The specimens were ultramicrotomed using a Reichert–Jug 'Ultracut' equipped with a diamond knife. The sections (~100 nm in thickness) were collected in a trough filled with water and then placed on a 200 mesh copper grid.

Scanning electron microscopy (SEM) imaging on tensile fractured surfaces was performed using a Zeiss Ultra Scanning Electron Microscope (for R-PE materials) or on a Tescan MIra Variable Pressure Field Emission Scanning Electron Microscope (for R-PS materials) at a voltage of 5.0 kV. Prior to being analysed the samples were mounted on stubs and their surface were platinum or gold coated.

Thermogravimetric analysis (TGA) was performed on a Perkin Elmer Pyrus 1 TGA equipped with an ultra-micro balance with a sensitivity of 0.1 μg, under nitrogen flow (20 $mL \cdot min^{-1}$), from 100 °C to 650 °C at a heating rate of 10 $°C \cdot min^{-1}$.

The tensile tests were run according to ISO 527:1996 on a Zwick Z005 machine (Germany). Five dog bone specimens (Type 1BA) were tensile tested using a 5 kN load cell and a testing speed of 20 $mm \cdot min^{-1}$ for R-PE materials and a 2.5 kN load cell and a testing speed of 5 $mm \cdot min^{-1}$ for R-PS materials. Impact tests were run according to standard ISO 179:1997 at room temperature on a Charpy impact tester (JinJian XJJD-5, China). The tests were run at a speed of 2.9 $m \cdot s^{-1}$ and using a hammer of 2 J for R-PE materials and 0.5 J for R-PS materials. Seven specimens (80 mm×10 mm×4 mm,

139 length×width×thickness) were impact tested for each batch of materials. Prior to being tested the impact
140 specimens were notched with a type A notch, using a 45º cutter and a milling machine. The mean and
141 standard deviation values reported for the mechanical tests represent a confidence level of 95%. Statistical
142 significance was assessed by a Two-tailed, Type II 't' test with a criterion that the probability of a
143 difference in means due to chance is smaller than 0.05.

144 **3 Results and discussion**

145 **3.1 Structure**

146 The XRD traces presented in Fig 1A show that the untreated organomodified montmorillonite
147 (Curve 1) presented a broad diffraction peak at a 2θ value of 3.3° which corresponds to a basal spacing,
148 $d_{(001)}$, of 2.7 nm.(Istrate et al., 2012) By treating the organomodified montmorillonite with the organic
149 blowing agent, the diffraction peak shifted towards a higher 2θ value. The intercalation of ADC inside the
150 interlayer space and the positive shift which was attributed to the removal of some surfactant molecules
151 from the clay mineral interlayer space have been discussed in our previous works (Istrate and Chen, 2012;
152 Istrate and Chen, 2014).

153 The dispersion of Clay (Fig 1B, Curve B1) into R-PS shifted the *(001)* diffraction peak for Clay to
154 a lower 2θ value of 2.5°, corresponding to a $d_{(001)}$ of 3.5 nm. This indicated the formation of intercalated
155 nanostructures. However, as observed from Fig 1B, Curve B2, the XRD trace for the ADC-Clay in the R-
156 PS does not present any significant peaks, except for a small and broad diffraction peak at a 2θ value of
157 5°. This peak represented the *(002)* diffraction peak, which is located at the same position as the *(002)*
158 diffraction peak of Clay/R-PS nanocomposite. The absence of the *(001)* peak and the presence of small
159 and broad *(002)* peak could suggest that the dispersion of ADC-Clay in R-PS led to the formation of
160 highly exfoliated nanocomposites. However, this could also arise from the orientation effect due to
161 sample preparation via hot pressing (Chen, 2005). This will be sequentially discussed from the TEM
162 images.

163

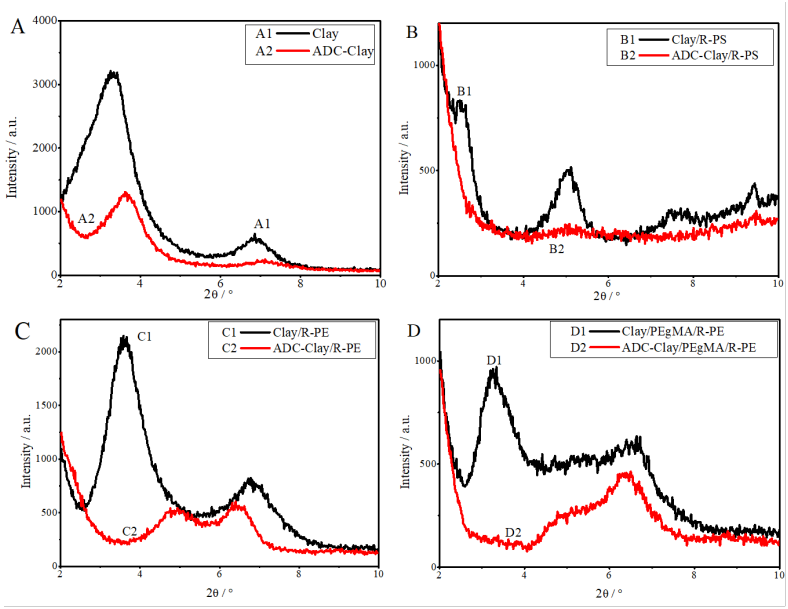

Fig. 1 XRD profiles of A) clay minerals (Istrate and Chen, 2014), and B) clay/R-PS, C) clay/R-PE and D) clay/PEgMA/R-PE composites and nanocomposites.

By dispersing Clay in R-PE (Fig 1C, Curve C1) the *(001)* diffraction peak shifted to slightly higher 2θ values indicating that conventional composites have formed. This is similar to the findings reported for neat Clay/PP composites and attributed to the immiscibility between the polymer and the organomodified montmorillonite and/or the degradation of the surfactant during melt processing (Chen and Evans, 2008; Istrate and Chen, 2012; Istrate and Chen, 2014). Replacing the Clay with ADC-Clay, the XRD spectra (Fig 1C, Curve C2) showed no significant *(001)* diffraction peaks between the 2θ values of 2° and 4°, where the *(001)* peaks for Clay (Fig 1A, Curve A1), ADC-Clay (Fig 1A, Curve A2) and Clay/R-PE (Fig 1C, Curve C1) were previously encountered. This can be attributed to the orientation effect of the clay layers inside the polymer matrix. The ADC-Clay/R-PE XRD trace presented two significant peaks that can be attributed to the *(002)* and *(003)* diffraction peaks of the clay mineral. These higher order peaks suggest that a highly ordered layer structures may have formed (Delbem et al., 2010). The dispersion of Clay into maleated ethylene compatibilised recycled PE (PEgMA/R-PE) showed no shift in the *(001)* diffraction peak (Fig 1D, Curve D1). Similar to the ADC-Clay/R-PE XRD spectra (Fig 1D, Curve D2), the presence of blowing agent-treated organomodified montmorillonite in PEgMA/R-PE showed no significant *(001)* peaks between the 2θ values of 2° and 4°; however, it did show the high

order diffraction peaks *(002)* and *(003)*. The formation of composite or nanocomposite structures in ADC-Clay/R-PE and ADC-Clay/PEgMA/R-PE will be discussed below from the TEM images.

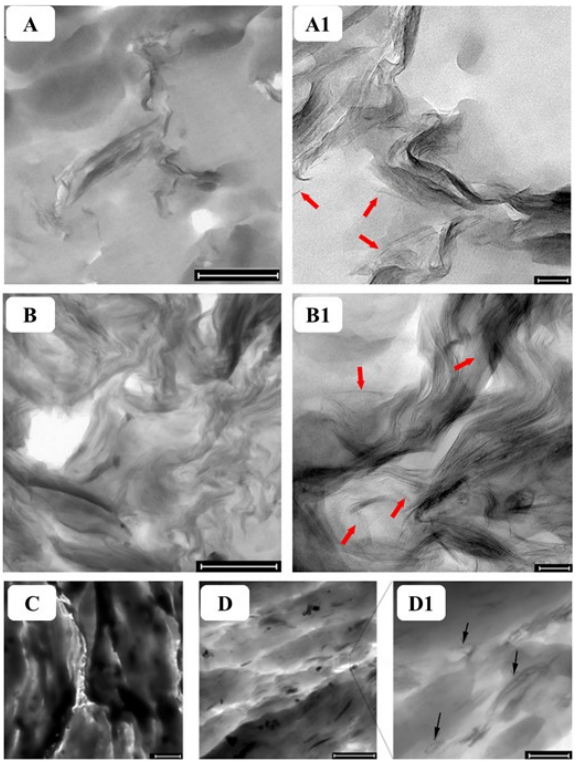

Fig. 2 TEM images of A. Clay/R-PS (Scale bar: 500 nm), A1. Clay/R-PS (Scale bar: 50 nm, the red arrows indicate single clay layers), B. ADC-Clay/R-PS (Scale bar: 500 nm), B1. ADC-Clay/PS (Scale bar: 50 nm, the red arrows indicate single clay layers), C. ADC-Clay/R-PE (Scale bar: 2 µm), D. ADC-Clay/PEgMA/R-PE (Scale bar: 1 µm) and D1. ADC-Clay/PEgMA/R-PE (Scale bar: 200 nm; the black arrows indicate the presence of voids between the clay layers). (For interpretation of the references to colour in this figure legend, the reader is referred to the web version of the article)

The intercalated nanostructures observed *via* XRD for clay/R-PS were confirmed by TEM (Fig 2A and 2A1). As observed from the XRD (Fig 1B) the addition of Clay (Curve B1) resulted in the formation of mostly intercalated clay nanostructures (Fig 2A). From the TEM images it was assessed that the intercalated mass fraction of nanostructures represented 87%, whilst only 13% of the nanostructures presented as exfoliated clay layers (determined from over 80 nanostructures). The intercalated clay tactoids presented between 2 and 12 clay layers per stack with an average of 3.9 clay layers per stack. The structure of ADC-Clay/R-PS was investigated via TEM (Fig 2B and 2B1). The fraction of exfoliated clay layers was determined to be 43%, whilst 57% of nanostructures were found to be intercalated clay

199 tactoids (determined from over 80 nanostructures). The intercalated nanostructures exhibited between 2
200 and 7 clay layers per stack with an average of 3.2 clay layers per stack. Using a blowing agent treated
201 organomodified montmorillonite resulted in more exfoliated clay/R-PS nanocomposites, which is in good
202 agreement with our previous findings on neat PS (Istrate and Chen, 2014). Typically,
203 intercalated/exfoliated nanostructures occur inside melt processed nanocomposites due to the shear forces
204 that are present during melt blending and the interfacial interactions between the polymer matrix and clay
205 minerals (Fornes and Paul, 2003; Paul and Robeson, 2008). When a chemical blowing agent is present
206 inside the interlayer space during melt mixing and heat exposure the blowing agent degrades forming
207 bubbles pushing the clay layers further apart (Istrate and Chen, 2014). The bubbles, gas molecules that
208 formed during heat decomposition of the blowing agent (Istrate and Chen, 2012), present as voids in the
209 TEM images (Fig 2D1).

210 The TEM images of ADC-Clay/R-PE (Fig 2C) showed that the absence of the *(001)* diffraction
211 peak from the XRD traces (Fig 1C, Curve C2) was due to the formation of conventional composites.
212 Similarly, the TEM representative images for compatibilised ADC-Clay/PEgMA/R-PE (Fig 2D) showed
213 that although the clay mineral was well dispersed in the polymer matrix, the reinforcement was mainly
214 made up by clay particles with intercalated clay tactoids being marginally identified. Thus, from the XRD
215 traces and the representative TEM images it was concluded that the dispersion of organomodified
216 montmorillonite and ADC-treated organomodified montmorillonite in compatibilised and un-
217 compatibilised R-PE resulted in the formation of conventional composites. This was due to the non-polar
218 character of R-PE and the possibility of having different polymer grades, additives and impurities present
219 into the recycle stock used. Although PEgMA was used as a compatibiliser, conventional composites
220 were obtained; this may be due to the compatibiliser content that may not have been enough to create an
221 interface between clay minerals and R-PE and the possible impurities that may be present in the recycling
222 stock.

223 **3.2 Thermal properties**

224 The thermal degradation temperature (measured as the peak temperature on the differential
225 thermogravimetric curves, Fig 3) showed different variations according to the type of recycled polymer
226 matrix, the type of clay mineral used and the presence or absence of the compatibilising agent. From Fig

3A it can be observed that the dispersion of clay minerals (Curve A2 and Curve A3 vs. Curve A1) led to no change in the thermal degradation temperature of R-PS. Typically, the dispersion of an organomodified montmorillonite into a polymer matrix leads to two effects: a catalysis effect, due to the presence of the surfactant which upon heat exposure decomposes, and a barrier effect, due to the presence of clay layers and clay tactoids which delay the volatilisation of the gases produced by the decomposition of the surfactant (Araujo et al., 2007; Gilman, 1999; Gilman et al., 2000; Xu et al., 2010). From the TGA traces for clay/R-PS it can be observed that these two opposite effects cancelled each other leading to no significant change in the thermal degradation temperature.

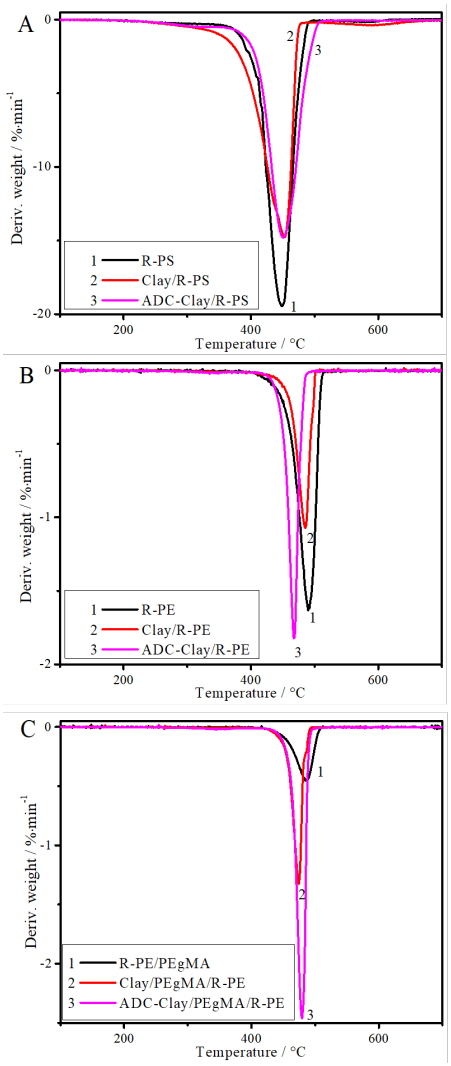

Fig. 3 Differential thermogravimetric profiles of A) clay/R-PS, B) clay/R-PE and C) clay/PEgMA/R-PE composites and nanocomposites.

239 The dispersion of Clay in R-PE resulted in a slight decrease in the thermal degradation temperature
240 (Fig 3B, Curve B2), whilst the presence of ADC-Clay in R-PE exhibited a prominent negative shift in the
241 thermal degradation temperature form 491 °C in R-PE (Fig 3B, Curve B1) to 468 °C (Fig 3B, Curve B3).
242 This can be due to poor dispersion of the clay layers inside the polymer matrix. Compared to R-PE or
243 PEgMA/R-PE the thermal degradation temperature of Clay/PEgMA/R-PE and ADC-Clay/PEgMA/R-PE
244 (Fig 3C) was found to diminish by up to 17 °C. The further exposure of the surfactant resulted into a
245 catalysis effect that dominated and facilitated the degradation of the recycled material. These results are
246 in good agreement with the findings previously reported for clay/PP composites (Istrate and Chen, 2014)

247

248 **3.3 Mechanical properties**

249 The dispersion of Clay and ADC-Clay in R-PS increased the Young's modulus, with statistical
250 significance, by 41% and 35% (Fig 4A). These enhancements can be attributed to the presence of
251 intercalated and exfoliated nanostructures inside the polymer matrix. The well dispersed single layers and
252 few-layer clay tactoids are characterised by a higher modulus than the clay particles which leads to stiffer
253 materials. The addition of organomodified montmorillonite or ADC-treated organomodifed
254 montmorillonite into R-PE and PEgMA/R-PE resulted in statistically significant enhancements in the
255 Young's modulus of up to 36% without the presence of a compatibilising agent and up to 47% in the
256 presence of PEgMA compared to R-PE. As opposed to the stiffness of PEgMA/R-PE, the dispersion of
257 the as-received organomodified montmorillonite and the blowing agent-treated organomodified
258 montmorillonite led to up to 34% statistically significant improvements. In this case the reinforcement
259 was represented by clay particles that were characterised by a superior stiffness compared to the polymer
260 matrix.

261 The addition of clay minerals improved the ultimate tensile strength (Fig 4B) of R-PS and R-PE.
262 The enhancements were between 12 and17% for R-PE and R-PS with Clay. However, when clay minerals
263 were added to compatibilised R-PE, the changes were insignificant. Elongation at break (Fig 4C) showed
264 depreciations compared to the neat recycled polymer for R-PS and R-PE, regardless of the clay mineral
265 used. This can be attributed to the brittle character of R-PS and to the formation of conventional
266 composites in the case of noncompatibilised R-PE. However, when clay minerals were added to
267 PEgMA/R-PE improvements close to 500% were observed compared to the compatibilised R-PE. The

268 improvements occurred due to the formation of intercalated clay/polymer nanocomposites and to the
269 mobility, dispersion and compatibilising effect of the clay tactoids (Chen and Evans, 2008; Dasari et al.,
270 2007).The changes in toughness observed during tensile testing (calculated as the energy absorbed by the
271 system before the breaking point) (Chen and Evans, 2009) and impact testing are depicted in Fig 4D.
272 Regardless of the type of clay mineral dispersed in R-PS, the tensile energy absorbed at break was found
273 to decrease by 72-77%. Similarly, the tensile energy at break of R-PE reduced with the addition of either
274 Clay or ADC-Clay. The reductions are due to the embrittlement effect of the clay mineral, as previously
275 reported in literature (Cotterell et al., 2007). However, compared to PEgMA/R-PE, the presence of Clay
276 and ADC-Clay led to statistically significant enhancements in the tensile energy at break by 458-463%.
277 The remarkable increases that occurred in the compatibilised R-PE with the addition of clay minerals can
278 be attributed to the dispersion, mobility and compatibilising effect of montmorillonite. The clay minerals,
279 in the presence of the maleated component, acted as a compatibilising agent between the different
280 polymer grades. Compared to the noncompatibilised clay/R-PE composites, clay/PEgMA/R-PE
281 composites presented a better dispersion of the clay particles (Fig 2D). Thus, the homogeneous dispersion
282 of clay particles in clay/PEgMA/R-PE resulted in improved tensile properties as opposed to the
283 noncompatibilised clay/R-PE composites. As shown in Fig 4D, the impact strength of the recycled
284 plastics decreased with statistical significance, regardless of the type of clay mineral used. However,
285 ADC-Clay/R-PS showed a 93% statistically significant improvement in impact strength compared to
286 Clay/R-PS. This enhancement may be attributed to better dispersion of nanostructures and an increase in
287 the degree of exfoliation from 13% to 43% as previously discussed. As it can be observed from Fig 4D,
288 only recycled impact-modified ADC-Clay/PS showed superior impact strength compared to Clay/R-PS;
289 the other materials presented reductions that were within the error.

290 The effect of dispersing organomodified montmorillonite or blowing agent-treated organomodified
291 montmorillonite in R-PS, R-PE or PEgMA/R-PE was investigated *via* SEM by analysing the impact
292 fractured surfaces of the recycled polymers and clay/polymer composites and nanocomposites. The
293 dispersion of clay minerals in R-PS (Fig 5A1 and 5A2) led to the formation of a rougher surface
294 compared to neat R-PS (Fig 5A). However, the presence of Clay resulted in a material that exhibited
295 some smoother areas compared to ADC-Clay/R-PS nanocomposites, which is in good agreement with the
296 lower impact strength observed for the former. The R-PE (Fig 5B) presented a vein-type pattern with a

fibrillar aspect, in which the addition of the compatibilising agent led to a change in the fibrillar and vein-type pattern density (Fig 5C), which is in accordance with the decrease in the toughness (estimated as the tensile energy at break during the tensile test or as the impact strength determined from the Charpy impact test). The conventional composites obtained by dispersing Clay in R-PE showed a fibrillar pattern and some smooth areas that were due to the embrittlement phenomenon that the clay layers induced (Cotterell et al., 2007). The dispersion of ADC-Clay in R-PE led to the formation of longer fibrils which is in good agreement with the higher energy absorbed at break that was observed *via* tensile testing for ADC-Clay/R-PE in comparison to Clay/R-PE. Similarly, the presence of clay minerals in maleated R-PE also resulted in the occurrence of highly fibrillar impact surfaces.

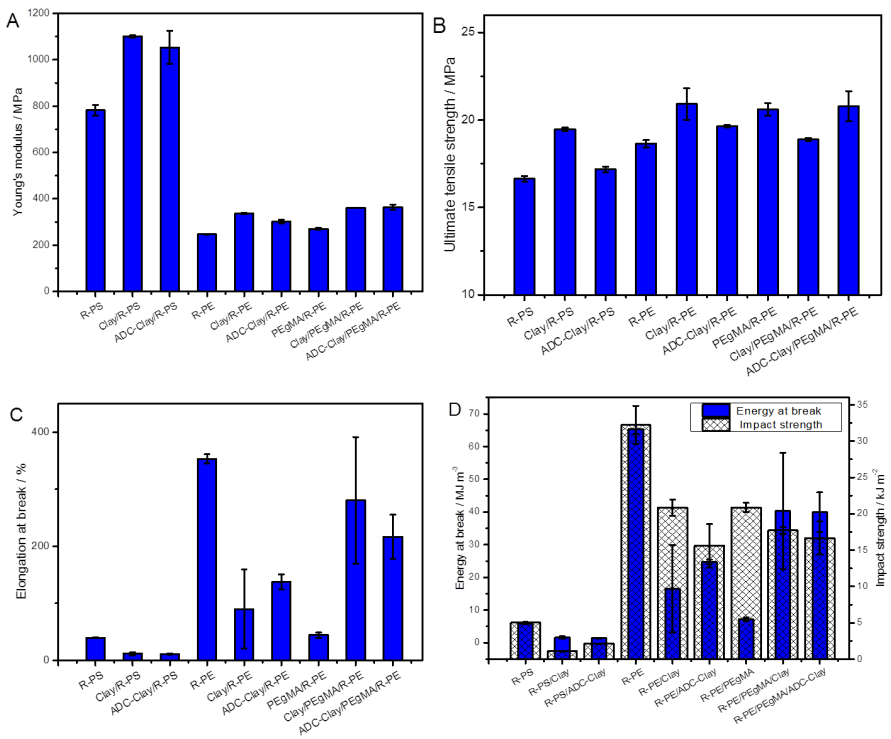

Fig. 4 A) Young's modulus for clay/R-PS nanocomposites and compatibilised and noncompatibilised clay/R-PE, B) ultimate tensile strength of clay/R-PS and compatibilised and noncompatibilised clay minerals/R-PE, C) elongation at break of clay/R-PS and compatibilised and noncompatibilised clay minerals/R-PE and D) toughness of clay/R-PS nanocomposites and compatibilised and noncompatibilised clay/R-PE composites (the bars represent averages of five measurements; the error bars represent ± standard deviation)

The intercalated/exfoliated ADC-Clay/R-PS nanocomposites in which the ratio of intercalated clay tactoids to exfoliated clay layers was close to unity presented a substantial increase in the impact strength compared to the highly intercalated Clay/R-PS nanocomposite. It has been previously reported in literature (Dasari et al., 2007) that a highly intercalated clay/nylon 6 nanocomposite presented a moderate increase in the impact strength compared to a highly exfoliated clay/nylon 6 nanocomposite. The ratios of the intercalated structures to the exfoliated structures presented in this work and the work from Dasari et al. (2007) are rather different, which may be a key reason for these different observations. Other reasons may include different clay minerals, polymers and interfacial interactions in both types of clay/polymer nanocomposites. In the current study, the improvement observed in the impact strength of the material with intercalated/exfoliated nanostructures over the one with mostly intercalated nanostructures may be due to enhanced exfoliation and exposure of the surfactant which may interact with the impact additives in the R-PS and improve the toughness of the system. The rougher fracture surface of ADC-Clay/R-PS nanocomposite compared to the slightly smoother fracture surfaces of Clay/R-PS nanocomposite were in good agreement with the impact strength data. However, the clay/R-PS nanocomposites present little variation in the tensile energy at break suggesting that presence of impact additives may interfere with the movement of the exfoliated clay layers during the tensile tests.

Unlike the clay/R-PS nanocomposites, ADC-Clay/R-PE microcomposite presented a reduction in the impact strength compared to Clay/R-PE microcomposite, whereas the tensile energy at break presented the opposite variation. This can be attributed to the smaller clay aggregates that form when the ADC-Clay was dispersed in R-PE. The enhanced impact strength of Clay/R-PE over ADC-Clay/R-PE may be a consequence of aggregates presence that once encountered on the crack path may force the crack to deviate and thus increase the energy absorbed by the system during the crack propagation. This difference may also be due to the different testing speeds that are used in impact tests compared to tensile tests, which was previously discussed in literature (Chen and Evans, 2008; Chen and Evans, 2009). In contrast, the presence of a compatibilising agent in the clay/R-PE conventional systems led to similar variations in the impact strength and tensile energy at break, presumably due to the larger clay microparticles present in these systems.

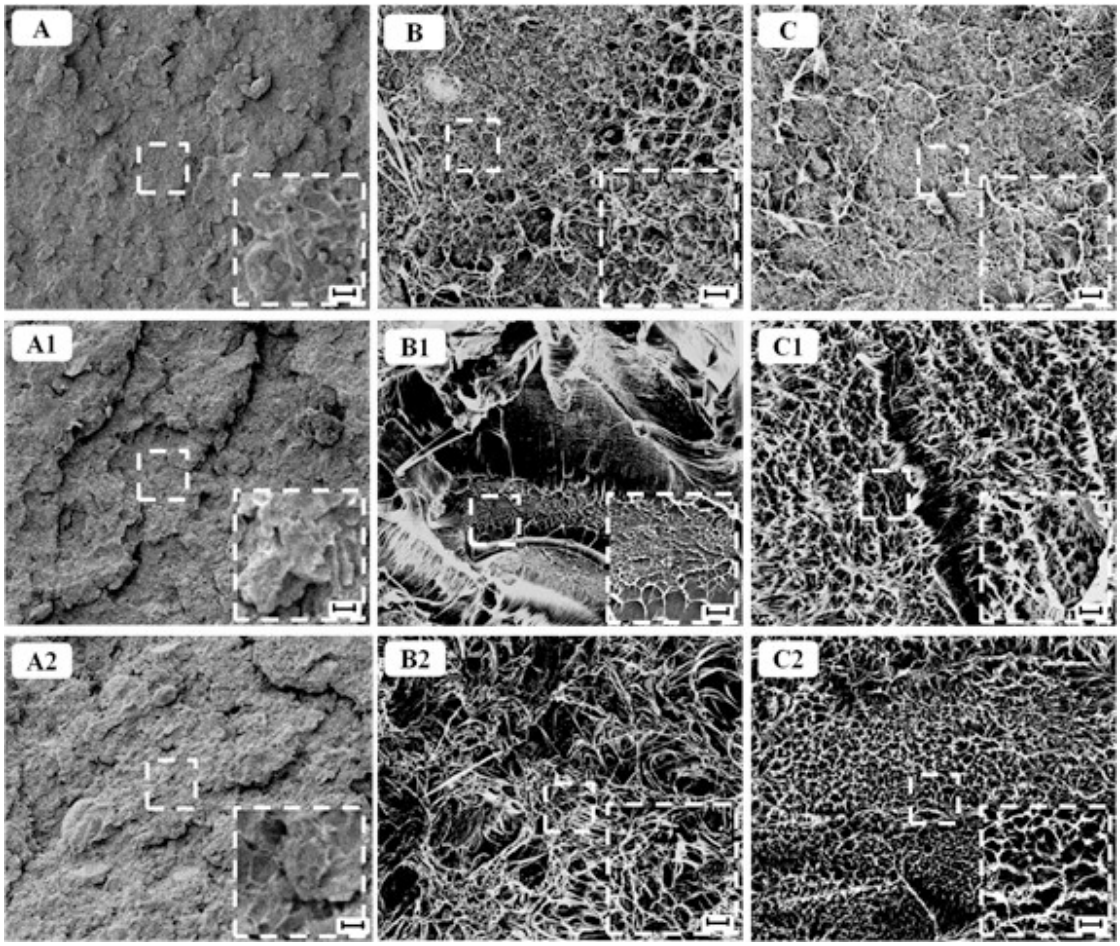

Fig. 5 SEM images: A. R-PS, A1. Clay/R-PS and A2. ADC-Clay/R-PS; B. R-PE, B1. Clay/R-PE and B2. ADC-Clay/R-PE; C. PEgMA/R-PE, C1. Clay/PEgMA/R-PE, and C2. ADC-Clay/PEgMA/R-PE (Scale bars for the main figures: 10 μm; and for the insets: 1 μm).

Although there are differences between neat PE and R-PE and neat PS and R-PS, owing mostly to the presence of impurities in the recycled materials, the changes observed in the mechanical properties with the addition of clay to R-PS and compatibilised and noncompatibilised R-PE are in good agreement with the changes observed for neat PE, compatibilised PE and neat PS (Istrate, 2012; Istrate and Chen, 2014). Clay/R-PS and ADC-Clay/R-PS presented superior stiffness compared to R-PS; however, the toughness of both nanocomposites decreased. In these cases the addition of clay embrittled the material. The compatibilised and noncompatibilised clay/R-PE microcomposites presented higher Young's moduli compared to the R-PE and PEgMA/R-PE. However, the toughness of clay/R-PE systems decreased regardless of the testing method. Unlike clay/R-PE systems, the presence of a compatibilising agent resulted in enhanced tensile energy at break and small reductions in the impact strength. The superior

stiffness and improved toughness attained with the dispersion of clay minerals in a compatibilised R-PE matrix suggest the potential that the dispersion of a small amount of clay layers in a recycled polymer matrix has.

4 Conclusions

The dispersion of Clay and ADC-Clay in R-PS led to the formation of intercalated/exfoliated clay/polymer nanocomposites. By dispersing the same clay minerals in R-PE with or without the addition of a compatibilising agent, conventional composites were formed. The highly non-polar character of the matrix, even with the introduction of the compatibilising agent, obstructed the delamination of the clay particles.

The presence of montmorillonite in R-PS only marginally improved the thermal degradation temperature of the material. However, the dispersion of Clay and ADC-Clay decreased the thermal degradation temperatures of the compatibilised and noncompatibilised R-PE. In this case, the catalytic effect of the surfactant dominated.

By dispersing Clay or ADC-Clay in the recycled materials the stiffness improved. The energy at break of the PEgMA/R-PE, assessed from the tensile tests, was found to significantly increase with the addition of montmorillonite. This may be due to the ability of clay to act, in the presence of a maleated component, as a compatibilising agent between different polymer grades and to the mobility of clay layers during the slow-speed testing. The superiority of the ADC-Clay over Clay was emphasised by a 93% increase in the impact strength of R-PS.

The presence of clay minerals generally improved the mechanical properties of the recycled materials. Although the thermal degradation temperature was reduced; this procedure, with some further optimisations, still has potential to help reuse recycled materials and ease the unavoidable polymer feedstock recuperation process.

Acknowledgements

The authors are grateful to the Environmental Protection Agency for supporting this work under research grant no. EPA-2008-PhD-WRM-4. Eoin Kearney is thanked for helping with sample preparation and

testing. The Conway Institute is thanked for aiding with the sample ultramicrotoming and facilitating access to the TEM instrument.

References

Araujo, E.M., Barbosa, R., Rodrigues, A.W.B., Melo, T.J.A., Ito, E.N., Processing and characterization of polyethylene/Brazilian clay nanocomposites. *Mater. Sci. Eng. A* **445**, 2007, 141-147.

Chaiko, D.J., Leyva, A.A., Thermal transitions and barrier properties of olefinic nanocomposites. *Chem. Mat.* **17**, 2005, 13-19.

Chen, B., Polymer-clay Nanocomposites, 2005, The University of London.

Chen, B., Evans, J.R.G., Nominal and effective volume fractions in polymer-clay nanocomposites. *Macromolecules* **39**, 2006, 1790-1796.

Chen, B., Evans, J.R.G., Impact and tensile energies of fracture in polymer-clay nanocomposites. *Polymer* **49**, 2008, 5113-5118.

Chen, B., Evans, J.R.G., Impact strength of polymer-clay nanocomposites. *Soft Matter* **5**, 2009, 3572 - 3584.

Cotterell, B., Chia, J.Y.H., Hbaieb, K., Fracture mechanisms and fracture toughness in semicrystalline polymer nanocomposites. *Eng. Fract. Mech*. **74**, 2007, 1054-1078.

Dasari, A., Yu, Z.-Z., Mai, Y.-W., Transcrystalline regions in the vicinity of nanofillers in polyamide-6. *Macromolecules* **40**, 2007, 123-130.

Delbem, M.F., Valera, T.S., Valenzuela-Diaz, F.R., Demarquette, N.R., Modification of a Brazilian smectite clay with different quaternary ammonium salts. *Química Nova* **33**, 2010, 309-315.

Finnveden, G., Johansson, J., Lind, P., Moberg, A., Life cycle assessment of energy from solid waste - part 1: general methodology and results. *J. Clean. Prod.* **13**, 2005, 213-229.

Fornes, T.D., Paul, D.R., Formation and properties of nylon 6 nanocomposites. *Polímeros* **13**, 2003, 212-217.

Fortelný, I., Michálková, D., Kruliš, Z., An efficient method of material recycling of municipal plastic waste. *Polym. Degrad. Stab*. **85**, 2004, 975-979.

Gilman, J.W., Flammability and thermal stability studies of polymer layered-silicate (clay) nanocomposites. *Appl. Clay Sci.* **15**, 1999, 31-49.

Gilman, J.W., Jackson, C.L., Morgan, A.B., Harris, R., Manias, E., Giannelis, E.P., Wuthenow, M., Hilton, D., Phillips, S.H., Flammability properties of polymer-layered-silicate nanocomposites. Polypropylene and polystyrene nanocomposites. *Chem. Mat*. **12**, 2000, 1866-1873.

Istrate, O.M., Polymer/Clay Nanocomposites, Mechanical and Manufacturing Engineering, 2012, University of Dublin, Trinity College Dublin.

Istrate, O.M., Chen, B., Porous exfoliated poly(ε-caprolactone)/clay nanocomposites: preparation, structure and properties. *J. Appl. Polym. Sci.* **125**, 2012, E102–E112.

Istrate, O.M., Chen, B., Enhancements of clay exfoliation in polymer nanocomposites using a chemical blowing agent. *Polym. Int*. **63**, 2014, 2008-2016.

Istrate, O.M., Gunning, M.A., Higginbotham, C.L., Chen, B., Structure-property relationships of polymer blend/clay nanocomposites: compatibilised and noncompatibilised polystyrene/propylene/clay *J. Polym. Sci. B Polym Phys* **50**, 2012, 431-441.

Kartalis, C.N., Papaspyrides, C.D., Pfaendner, R., Hoffmann, K., Herbst, H., Recycled and restabilized HDPE bottle crates: retention of critical properties after heat aging. *Polym. Eng. Sci.* **41**, 2001, 771-781.

Katti, K.S., Sikdar, D., Katti, D.R., Ghosh, P., Verma, D., Molecular interactions in intercalated organically modified clay and clay-polycaprolactam nanocomposites: experiments and modeling. *Polymer* **47**, 2006,403-414.

Lee, J.H., Song, D.I., Jeon, Y.W., Adsorption of organic phenojs onto dual organic cation montmorillonite from water. *Sep. Sci. Technol*. **32**, 1997, 1975-1992.

Liu, W., Gan, J., Papiernik, S.K., Yates, S.R., Sorption and catalytic hydrolysis of diethatyl-ethyl on homoionic clays. *J. Agric. Food Chem*. **48**, 2000, 1935-1940.

Okada, A., Usuki, A., Twenty years of polymer-clay nanocomposites (vol 291, 1449, 2006). *Macromol. Mater. Eng.* **291**, 2007, 1449-1476.

Paul, D.R., Robeson, L.M., Polymer nanotechnology: Nanocomposites. *Polymer* **49**, 2008, 3187-3204.

Pegoretti, A., Kolarik, J., Peroni, C., Migliaresi, C., Recycled poly(ethylene terephthalate)/layered silicate nanocomposites: morphology and tensile mechanical properties. *Polymer* **45**, 2004, 2751-2759.

Phuong, N.T., Gilbert, V., Chuong, B., Preparation of recycled polypropylene/organophilic modified layered silicates nanocomposites part I: the recycling process of polypropylene and the mechanical oroperties of recycled polypropylene/organoclay nanocomposites. *J. Reinf. Plast. Compos.* **27,** 2008, 1983-2000.

Pospíšil, J., Sitek, F.A., Pfaendner, R., Upgrading of recycled plastics by restabilization—an overview. *Polym. Degrad. Stab.* **48**, 1995, 351-358.

Quispe, N.B., Fernandes, E.G., Zanata, F., Bartoli, J.R., Souza, D.H., Ito, E.N., Organoclay nanocomposites of post-industrial waste poly(butylene terephthalate) from automotive parts. *Waste Manag. Res.* **33**, 2015, 908-918.

Strömberg, E., Karlsson, S., The design of a test protocol to model the degradation of polyolefins during recycling and service life. *J. Appl.Polym. Sci.* **112**, 2009, 1835-1844.

Vilaplana, F., Karlsson, S., Quality concepts for the improved use of recycled polymeric materials: a review. *Macromolec. Mater. Eng.* **293**, 2008, 274-297.

Xu, X., Ding, Y., Wang, F., Wen, B., Zhang, J., Zhang, S., Yang, M., Effects of silane grafting on the morphology and thermal stability of poly(ethylene terephthalate)/clay nanocomposites. *Polym. Compos.* **31**, 2010, 825-834.

Zhao, J., Morgan, A.B., Harris, J.D., Rheological characterization of polystyrene-clay nanocomposites to compare the degree of exfoliation and dispersion. *Polymer* **46**, 2005, 8641-8660.